Organic Electronics 14 (2013) 1516–1520

Contents lists available at SciVerse ScienceDirect

Organic Electronics

journal homepage: www.elsevier.com/locate/orgel

Letter

Megahertz operation of flexible low-voltage organic thin-film transistors

Ute Zschieschang [a,*], Robert Hofmockel [a], Reinhold Rödel [a], Ulrike Kraft [a], Myeong Jin Kang [b], Kazuo Takimiya [b], Tarek Zaki [c], Florian Letzkus [d], Jörg Butschke [d], Harald Richter [d], Joachim N. Burghartz [d], Hagen Klauk [a]

[a] Max Planck Institute for Solid State Research, Heisenbergstr. 1, 70569 Stuttgart, Germany
[b] Department of Applied Chemistry, Graduate School of Engineering, Institute for Advanced Materials Research, Hiroshima University, Higashi-Hiroshima, Japan
[c] Institute for Nano- and Microelectronic Systems (INES), University of Stuttgart, Germany
[d] Institut für Mikroelektronik/IMS CHIPS, Stuttgart, Germany

ARTICLE INFO

Article history:
Received 10 January 2013
Received in revised form 5 March 2013
Accepted 9 March 2013
Available online 31 March 2013

Keywords:
Organic thin-film transistors
Flexible organic circuits

ABSTRACT

Bottom-gate, top-contact (inverted staggered) organic thin-film transistors with a channel length of 1 μm have been fabricated on flexible plastic substrates using the vacuum-deposited small-molecule semiconductor 2,9-didecyl-dinaphtho[2,3-b:2′,3′-f]thieno[3,2-b]thiophene (C_{10}-DNTT). The transistors have an effective field-effect mobility of 1.2 cm^2/V s, an on/off ratio of 10^7, a width-normalized transconductance of 1.2 S/m (with a standard deviation of 6%), and a signal propagation delay (measured in 11-stage ring oscillators) of 420 ns per stage at a supply voltage of 3 V. To our knowledge, this is the first time that megahertz operation has been achieved in flexible organic transistors at supply voltages of less than 10 V.

Organic thin-film transistors (TFTs) are of interest for flexible, large-area electronics applications, such as rollable or foldable information displays [1–3], conformable sensor arrays [4], and plastic circuits [5,6]. In some of the more advanced applications envisioned for organic TFTs, such as the integrated row and column drivers of flexible active-matrix organic light-emitting diode (AMOLED) displays [7–9], the TFTs will have to be able to control electrical signals of a few volts at frequencies of several megahertz. In a few previous reports, megahertz operation has indeed been achieved in organic TFTs, but only when the transistors were fabricated on rigid glass or silicon substrates [10–15] or when the transistors were operated with relatively high voltages, between 10 and 25 V [5,10,12–14,16]. Here we demonstrate the first flexible organic TFTs and ring oscillators with switching frequencies above 1 MHz at supply zvoltages between 2 and 3 V. This range of supply voltages is expected to be useful for AMOLED displays, since it is the voltage range in which organic LEDs have shown the highest reported luminous efficiencies [17–19].

The first requirement for achieving high switching frequencies in field-effect transistors is efficient charge transport in the semiconductor. To meet this requirement we have chosen the organic semiconductor 2,9-didecyl-dinaphtho[2,3-b:2′,3′-f]thieno[3,2-b]thiophene (C_{10}-DNTT), which has previously shown field-effect mobilities up to 8 cm^2/V s in TFTs on smooth silicon substrates [20] and up to 4 cm^2/V s in TFTs on plastic substrates [21,22]. These mobilities are larger by a factor of about 2 than the mobilities reported for the non-alkylated parent compound DNTT [23,24]. Compared with DNTT, the attractive interactions between the decyl substituents of neighboring C_{10}-DNTT molecules within the semiconductor layer are believed to force the molecules into a tighter solid-state packing, leading to enhanced orbital overlap and thereby to enhanced charge-carrier transport in the plane parallel to the substrate surface [20,25].

* Corresponding author. Tel.: +49 71 1689 1401; fax: +49 71 1689 1472.
E-mail address: U.Zschieschang@fkf.mpg.de (U. Zschieschang).

1566-1199/$ - see front matter © 2013 Elsevier B.V. All rights reserved.
http://dx.doi.org/10.1016/j.orgel.2013.03.021

The second requirement for achieving high switching frequencies in field-effect transistors is a small channel length [5,10–16]. To meet this requirement we have employed high-resolution silicon stencil masks to pattern the gate electrodes, the organic semiconductor, and the source and drain contacts of the transistors, which makes it possible to fabricate bottom-gate, top-contact organic TFTs with a channel length of 1 μm without exposing the organic semiconductor layer to potentially harmful organic solvents and photoresists [26,27].

The TFTs and ring oscillators were fabricated on 125-μm-thick polyethylene naphthalate substrates (Teonex® Q65 PEN; kindly provided by William A. MacDonald, DuPont Teijin Films, Wilton, UK). To prepare the gate electrodes, 20-nm-thick aluminum was deposited directly onto the PEN substrates by thermal evaporation in vacuum through a first stencil mask. In order to define the locations for the gate vias, 20-nm-thick gold was then deposited by thermal evaporation in vacuum through a second stencil mask onto specific locations on the aluminum outside of the active TFT areas. In the third step, a hybrid gate dielectric composed of a 3.6-nm-thick layer of aluminum oxide (obtained by briefly exposing the surface of the aluminum gate electrodes to an oxygen plasma) and a 1.7-nm-thick self-assembled monolayer (SAM) of *n*-tetradecylphosphonic acid (obtained by immersing the substrate into a 2-propanol solution of the phosphonic acid) was then formed [21,24]. This gate dielectric is formed only on the surface of the aluminum gate electrodes, but not in the gold-covered via locations. In the fourth step, the organic semiconductor with a thickness of 20 nm is deposited onto the AlO_x/SAM gate dielectric by sublimation in vacuum through a third stencil mask. Finally, 30-nm-thick gold is deposited by thermal evaporation in vacuum through a fourth stencil mask to define the source and drain contacts of the TFTs as well as the interconnects for the ring oscillators. The small thickness (5.3 nm) and large capacitance per unit area (800 nF/cm^2) of the AlO_x/SAM gate dielectric allows the transistors and circuits to operate with low voltages of about 2–3 V [21]. The air stability, operational stability, bending stability and thermal stability of long-channel TFTs fabricated with this process have been analyzed previously [21,28,29]; here we will focus on the performance and parameter uniformity of transistors with aggressively reduced lateral dimensions.

Fig. 1 shows two photographs and the current–voltage characteristics of a C_{10}-DNTT TFT with a channel length of 1 μm and a channel width of 10 μm fabricated on a flexible PEN substrate. In the saturation regime, the TFT has an effective field-effect mobility of 1.2 cm^2/V s and an on/off ratio of 10^7, both of which are to our knowledge the largest reported thus far for an organic TFT with a channel length of 1 μm. The observation that the effective field-effect mobility in these short-channel TFTs is only about one third of the mobility reported for long-channel TFTs based on the same semiconductor [21,22] can be explained by the larger contribution of the contact resistance to the total device resistance when the channel length is significantly reduced [15,24,30].

Owing to the unique combination of a large gate-dielectric capacitance per unit area (800 nF/cm^2), a small channel length (1 μm), and a relatively large effective field-effect mobility (1.2 cm^2/V s), the width-normalized transconductance (i.e., the derivative of the measured drain current, I_D, versus the applied gate-source voltage, V_{GS}, normalized to the channel width, W: $g_m/W = (\partial I_D/\partial V_{GS})/W$) of these transistors reaches 1.2 S/m, which is to our knowledge the largest width-normalized transconductance reported thus far for an organic transistor fabricated on a plastic substrate. For comparison, the width-normalized transconductance

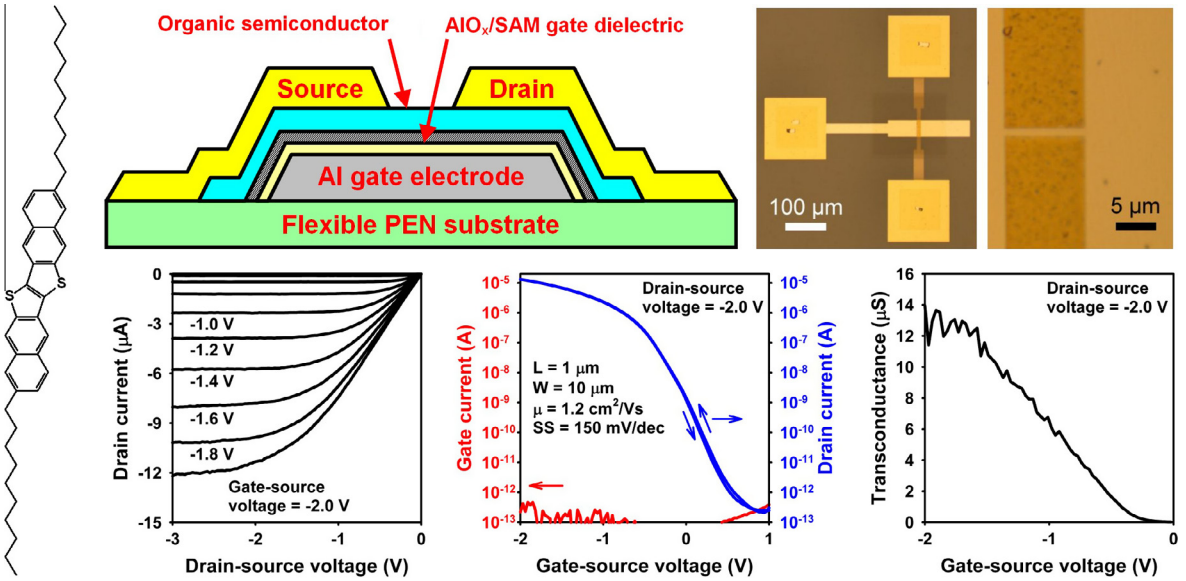

Fig. 1. Schematic cross-section, photographs, and electrical characteristics of a C_{10}-DNTT TFT with a channel length of 1 μm fabricated on a flexible PEN substrate. The TFT has an effective field-effect mobility of 1.2 cm^2/V s, an on/off current ratio of 10^7, a subthreshold swing of 150 mV/decade, and a width-normalized transconductance of 1.2 S/m. Also shown is the chemical structure of the organic semiconductor, C_{10}-DNTT.

of the high-mobility (30 cm^2/V s) organic single-crystal FETs reported by Minemawari et al. [31] is about 0.04 S/m, that of the self-aligned polymer TFTs with an extremely short channel length of 200 nm reported by Noh et al. [11] is about 0.05 S/m, and that of the flexible high-performance pentacene TFTs with a photolithographically defined channel length of 2 μm recently reported by Myny et al. [5] is about 0.3 S/m. The main reason why a large transconductance is desirable is that it is one of only two parameters that determine the maximum frequency, f_T, at which a field-effect transistor can be operated; the other being the gate capacitance, C_G: $f_T = g_m/(2\pi C_G)$ [32].

Fig. 2 shows the measured transfer characteristics and the distribution of the extracted width-normalized transconductance in an array of sixteen C_{10}-DNTT TFTs with a nominal channel length of 1 μm and a nominal channel width of 10 μm fabricated on a flexible PEN substrate. As can be seen, all 16 TFTs have an on/off ratio of about 10^7. Across the array of 16 TFTs, the width-normalized transconductance varies between a minimum of 1.16 S/m and a maximum of 1.40 S/m, with a standard deviation of 6%. Note that the width-normalized transconductance of a field-effect transistor is always inversely proportional to the channel length, L: $g_m/W = \mu_{eff} C_{diel} V_{DS}/L$; where μ_{eff} is the effective field-effect mobility, C_{diel} is the gate-dielectric capacitance per unit area, and V_{DS} is the drain-source voltage. Therefore, assuming that the effective field-effect mobility and the dielectric capacitance are constant across the substrate, a standard deviation in the transconductance of 6% may simply reflect a standard deviation in the channel length of 6%, which in the case of an intended channel length of 1 μm would correspond to a standard deviation of 60 nm. For comparison, the standard deviation of the gate length of silicon metal-oxide-semiconductor field-effect transistors (MOSFETs) at the 32-nm technology node is much smaller, less than 10 nm [33]. However, the transistor patterns in these state-of-the-art silicon MOSFETs are defined by reduction projection lithography, which means that the features drawn on the photomask are more relaxed (usually by a factor of 4 or 5) than the features reproduced on the wafer, which can be helpful in keeping variations small. In contrast, organic TFTs (including those reported here) are usually fabricated without pattern reduction, i.e., the mask features are reproduced 1:1 onto the substrate. Under these circumstances, and also considering the surface roughness of the plastic substrate, a standard deviation of 60 nm in the channel length may already be approaching the best achievable uniformity for flexible organic transistors.

The third and final requirement for achieving high switching frequencies (in addition to a large field-effect mobility and a small channel length, as discussed above) is a small gate capacitance. The gate capacitance has two components: an intrinsic component and a parasitic component: The intrinsic component is the capacitance of the channel area (given by the product of the channel length, L, and the channel width, W), while the parasitic component is the capacitance of the areas in which the source and drain contacts overlap the gate electrode: $C_G = C_{diel}(-L + 2L_C)W$, where L_C is the gate overlap (or contact length). Therefore, in view of high-frequency transistor operation it can be useful to reduce not only the channel length L, but also the gate overlap L_C [5,10–16]. For example, when L = 1 μm, L_C = 5 μm, W = 10 μm and C_{diel} = 800 nF/cm^2, the calculated gate capacitance is 0.9 pF, which corresponds to a width-normalized gate capacitance, C_G/W, of 90 nF/m. Further assuming a width-normalized transconductance of 1.2 S/m, we project a maximum frequency of 2 MHz and a minimum signal delay, $\tau = 1/(2f_T)$, of 250 ns.

Fig. 3 shows the circuit schematic and the photograph of an 11-stage ring oscillator comprised of unipolar inverters fabricated using high-resolution silicon stencil masks on a flexible PEN substrate. In the most aggressive design, the TFTs have a channel length of 1 μm, a gate overlap of 5 μm, and channel widths of 24 μm (for the drive TFTs) or 72 μm (for the load TFTs). In a more relaxed design, the channel length is 4 μm and the gate overlap is 20 μm. Also shown are the signal propagation delays per stage measured with these ring oscillators and plotted as a function of the supply voltage. For the more aggressive dimensions (L = 1 μm, L_C = 5 μm), the measured stage delay is 1.9 μsec at a supply voltage of 1 V, 730 ns at 2 V, 420 ns at 3 V, and 300 ns at 4 V. This is within a factor of two or three of the theoretically predicted delay (see

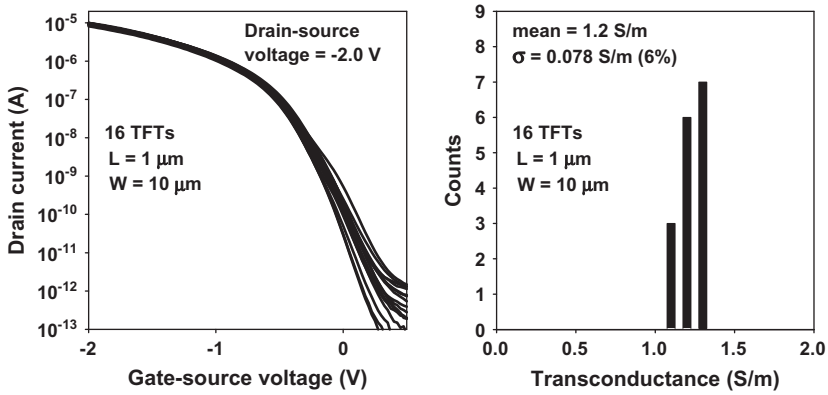

Fig. 2. Distribution of the measured transfer characteristics and distribution of the width-normalized transconductance in an array of 16 C_{10}-DNTT TFTs with a channel length of 1 μm fabricated on a flexible PEN substrate.

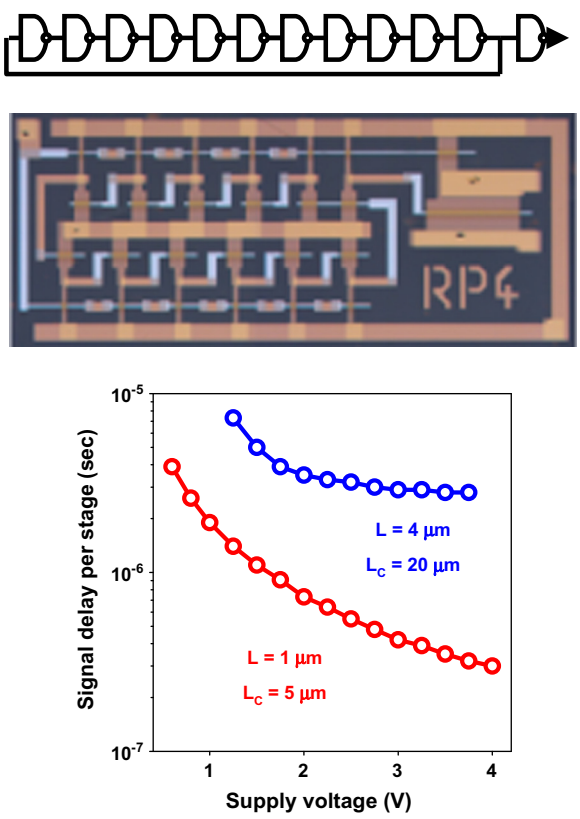

Fig. 3. Circuit schematic, photograph and measured signal propagation delay per stage as a function of the supply voltage of 11-stage unipolar ring oscillators fabricated with C_{10}-DNTT TFTs with two different channel lengths (1 μm and 4 μm) on a flexible PEN substrate. For a channel length of 1 μm, the measured stage delay is 1.9 μsec at a supply voltage of 1 V, 730 ns at a supply voltage of 2 V, 420 ns at a supply voltage of 3 V, and 300 ns at a supply voltage of 4 V.

above) and represents to our knowledge the best dynamic performance reported thus far for flexible organic ring oscillators at supply voltages of less than 10 V. For larger supply voltages of 10–20 V, the IMEC group has measured record signal delays as short as 190 ns per stage in flexible organic ring oscillators [5,16], and Nakahara et al. have estimated a signal delay of 140 ns from the response of an individual submicron organic transistor to a square-wave input signal [34]. For organic ring oscillators fabricated on glass, Ante et al. have measured a signal delay of 230 ns per stage at a supply voltage of 4.2 V [15]. For complementary circuits, which comprise *p*-channel and *n*-channel organic TFTs and thus have important advantages over unipolar circuits in terms of signal integrity and static power consumption [35,36], the best reported signal delays are as short as 500 ns per stage on glass substrates and 10 μsec on flexible plastic substrates [14,36–41].

In summary, we have fabricated low-voltage organic thin-film transistors and ring oscillators based on the organic semiconductor 2,9-didecyl-dinaphtho [2,3-b:2′,3′-f]thieno[3,2-b]thiophene (C_{10}-DNTT) on flexible plastic substrates. TFTs with aggressively reduced lateral dimensions ($L = 1$ μm) have a width-normalized transconductance of 1.2 S/m (with a standard deviation of 6%) and a signal propagation delay of 420 ns per stage at a supply voltage of 3 V. To our knowledge, this is the first time that megahertz operation has been achieved in flexible organic transistors at supply voltages of less than 10 V. Further improvements in the dynamic performance of organic TFTs may be possible by employing organic semiconductors with an even larger intrinsic field-effect mobility [42] and by further reducing the lateral TFT dimensions [43], ideally in combination with a thinner gate dielectric [44] and efficient, area-selective contact doping [45].

Acknowledgment

This work was partially funded by the German Research Foundation (DFG) under Grant KL 2223/5-1.

References

[1] M. Noda, N. Kobayashi, M. Katsuhara, A. Yumoto, S. Ushikura, R. Yasuda, N. Hirai, G. Yukawa, I. Yagi, K. Nomoto, T. Urabe, J. Soc. Inf. Display 19 (2011) 316.
[2] M.A. McCarthy, B. Liu, E.P. Donoghue, I. Kravchenko, D.Y. Kim, F. So, A.G. Rinzler, Science 332 (2011) 570.
[3] D. Braga, N.C. Erickson, M.J. Renn, R.J. Holmes, C.D. Frisbie, Adv. Funct. Mater. 22 (2012) 1623.
[4] T. Someya, Y. Kato, T. Sekitani, S. Iba, Y. Noguchi, Y. Murase, H. Kawaguchi, T. Sakurai, Proc. National Acad. Sci. 102 (2005) 12321.
[5] K. Myny, S. Steudel, S. Smout, P. Vicca, F. Furthner, B. van der Putten, A.K. Tripathi, G.H. Gelinck, J. Genoe, W. Dehaene, P. Heremans, Org. Electron. 11 (2010) 1176.
[6] K. Myny, E. van Veenendaal, G.H. Gelinck, J. Genoe, W. Dehaene, P. Heremans, IEEE J. Solid State Circ. 47 (2012) 284.
[7] L.Q. Zhao, C.Y. Wu, D.S. Hao, Y. Yao, Z.G. Meng, S.Z. Xiong, Optoelectron. Lett. 5 (2009) 104.
[8] B.D. Choi, C.W. Byun, IEEE Trans. Consumer Electron. 56 (2010) 1102.
[9] P. Schalberger, M. Herrmann, S. Hoehla, N. Fruehauf, J. Soc. Inf. Display 19 (2011) 496.
[10] V. Wagner, P. Wöbkenberg, A. Hoppe, J. Seekamp, Appl. Phys. Lett. 89 (2006) 243515.
[11] Y.Y. Noh, N. Zhao, M. Caironi, H. Sirringhaus, Nature Nanotechnol. 2 (2007) 784.
[12] M. Kitamura, Y. Arakawa, Appl. Phys. Lett. 95 (2009) 023503.
[13] M. Kitamura, Y. Arakawa, Jpn. J. Appl. Phys. 50 (2011) 01BC01.
[14] M. Kitamura, Y. Kuzumoto, S. Aomori, Y. Arakawa, Appl. Phys. Express 4 (2011) 051601.
[15] F. Ante, D. Kälblein, T. Zaki, U. Zschieschang, K. Takimiya, M. Ikeda, T. Sekitani, T. Someya, J.N. Burghartz, K. Kern, H. Klauk, Small 8 (2012) 73.
[16] P. Heremans, J. Genoe, S. Steudel, K. Myny, S. Smout, P. Vicca, C. Grillberger, O.R. Hild, F. Furthner, B. van der Putten, A.K. Tripathi, G.H. Gelinck, IEEE International Electron Devices Meeting (IEDM) Technical Digest (2009).
[17] R. Meerheim, S. Olthof, M. Hermenau, S. Scholz, A. Petrich, N. Tessler, O. Solomeshch, B. Lüssem, M. Riede, K. Leo, J. Appl. Phys. 109 (2011) 103102.
[18] J. Birnstock, T. Canzler, M. Hofmann, A. Lux, S. Murano, P. Wellmann, A. Werner, J. Soc. Inf. Display 16 (2008) 221.
[19] N. Chopra, J.S. Swensen, E. Polikarpov, L. Cosimbescu, F. So, A.B. Padmaperuma, Appl. Phys. Lett. 97 (2010) 033304.
[20] M.J. Kang, I. Doi, H. Mori, E. Miyazaki, K. Takimiya, M. Ikeda, H. Kuwabara, Adv. Mater. 23 (2011) 1222.
[21] U. Zschieschang, M.J. Kang, K. Takimiya, T. Sekitani, T. Someya, T.W. Canzler, A. Werner, J. Blochwitz-Nimoth, H. Klauk, J. Mater. Chem. 22 (2012) 4273.
[22] I. Doi, M.J. Kang, K. Takimiya, Curr. Appl. Phys. 12 (2012) e2.
[23] T. Yamamoto, K. Takimiya, J. Am. Chem. Soc. 129 (2007) 2224.
[24] U. Zschieschang, F. Ante, D. Kälblein, T. Yamamoto, K. Takimiya, H. Kuwabara, M. Ikeda, T. Sekitani, T. Someya, J. Blochwitz-Nimoth, H. Klauk, Org. Electron. 12 (2011) 1370.
[25] M.J. Kang, E. Miyazaki, I. Osaka, K. Takimiya, Jpn. J. Appl. Phys. 51 (2012) 11PD04.
[26] F. Letzkus, J. Butschke, B. Höfflinger, M. Irmscher, C. Reuter, R. Springer, A. Ehrmann, J. Mathuni, Microelectron. Eng. 53 (2000) 609.

[27] K. Sidler, N.V. Cvetkovic, V. Savu, D. Tsamados, A.M. Ionescu, J. Brugger, Sens. Actuators, A 162 (2010) 155.
[28] T. Sekitani, U. Zschieschang, H. Klauk, T. Someya, Nature Mater. 9 (2010) 1015.
[29] K. Kuribara, H. Wang, N. Uchiyama, K. Fukuda, T. Yokota, U. Zschieschang, C. Jaye, D. Fischer, H. Klauk, T. Yamamoto, K. Takimiya, M. Ikeda, H. Kuwabara, T. Sekitani1, Y.L. Loo, T. Someya, Nature Commun. 3 (2012) 723.
[30] H. Klauk, U. Zschieschang, M. Halik, J. Appl. Phys. 102 (2007) 074514.
[31] H. Minemawari, T. Yamada, H. Matsui, J. Tsutsumi, S. Haas, R. Chiba, R. Kumai, T. Hasegawa, Nature 475 (2011) 364.
[32] S.M. Sze, K.K. Ng, Physics of Semiconductor Devices, third ed., John Wiley & Sons, 2007.
[33] A. Asenov, S. Kaya, A.R. Brown, IEEE Trans. Electr. Dev. 50 (2003) 1254.
[34] R. Nakahara, M. Uno, K. Takimiya, J. Takeya, Adv. Mater. 24 (2012) 5212.
[35] D. Bode, C. Rolin, S. Schols, M. Debucquoy, S. Steudel, G.H. Gelinck, J. Genoe, P. Heremans, IEEE Trans. Electr. Dev. 57 (2010) 201.
[36] B.K. Crone, A. Dodabalapur, R. Sarpeshkar, R.W. Filas, Y.Y. Lin, Z. Bao, J.H. O'Neill, W. Li, H.E. Katz, J. Appl. Phys. 89 (2001) 5125.
[37] B. Yoo, T. Jung, D. Basu, A. Dodabalapur, B.A. Jones, A. Facchetti, M.R. Wasielewski, T.J. Marks, Appl. Phys. Lett. 88 (2006) 082104.
[38] D. Bode, K. Myny, B. Verreet, B. van der Putten, P. Bakalov, S. Steudel, S. Smout, P. Vicca, J. Genoe, P. Heremans, Appl. Phys. Lett. 96 (2010) 133307.
[39] K.J. Baeg, D. Khim, D.Y. Kim, S.W. Jung, J.B. Koo, I.K. You, H. Yan, A. Facchetti, Y.Y. Noh, J. Polym. Sci., Part B: Polym. Phys. 49 (2011) 62.
[40] W. Smaal, C. Kjellander, Y. Jeong, A. Tripathi, B. van der Putten, A. Facchetti, H. Yan, J. Quinn, J. Anthony, K. Myny, W. Dehaene, G. Gelinck, Org. Electron. 13 (2012) 1686.
[41] D.E. Schwartz, T.N. Ng, IEEE Electr. Dev. Lett. 34 (2013) 271.
[42] A.Y. Amin, A. Khassanov, K. Reuter, T. Meyer-Friedrichsen, M. Halik, J. Am. Chem. Soc. 134 (2012) 16548.
[43] T. Zaki, R. Rödel, F. Letzkus, H. Richter, U. Zschieschang, H. Klauk, J.N. Burghartz, IEEE Electr. Dev. Lett. 34 (2013) 520.
[44] A. Jedaa, M. Burkhardt, U. Zschieschang, H. Klauk, D. Habich, G. Schmid, M. Halik, Org. Electron. 10 (2009) 1442.
[45] F. Ante, D. Kälblein, U. Zschieschang, T.W. Canzler, A. Werner, K. Takimiya, M. Ikeda, T. Sekitani, T. Someya, H. Klauk, Small 7 (2011) 1186.